International Journal of Applied Engineering Research ISSN 0973-4562 Volume 12, Number 24 (2017) pp. 14046-14053

An Intelligent Control System for Refrigeration Cycle Powered by Renewable Energy

Ayman A. Aly[a,b] and B. Saleh[a,b]

[a]Department of Mechanical Engineering, Faculty of Engineering, Taif University, P.O. Box 888, Al-Hawyah, Saudi Arabia.

[b]Department of Mechanical Engineering, Faculty of Engineering, Assiut University, Assiut, Egypt.

Abstract

The most critical problem in the world is to meet the energy demand, because of steadily increasing energy consumption. Refrigeration and air conditioning (R&AC) applications account for more than one third the total electrical use in homes and commercial buildings especially in hot countries like Saudi Arabia. This paper presents an effective technique to enhance the performance of a newly-developed Refrigeration Cycle Powered by Renewable Energy. In this design, presents the modeling and simulation of solar-powered desiccant regenerator used for open absorption cooling system. The implementation of a fuzzy logic controller for a solar powered air refrigeration system and its advantages are investigated in this paper. The proposed design is promising for an improvement of the system performance while fulfilling the cooling demand with guaranteed energy efficiency.

Keywords: Performance improvement, Solar-powered, fuzzy control, Absorption cooling, modeling, simulation.

NOMENCLATURE

A	constant in Eq. 12
A_c	collector surface area,m^2
a	transfer area, m^2/m^3
B	constant in Eq. 12
C	specific heat, J/kg K
H	specific enthalpy, J/kg
h	heat transfer coefficient, W/m^2 °C
I	solar radiation intensity, W/m^2
G	fluid mass velocity, kg/m^2 s
K_a	mass transfer coefficient, m/ s
L	latent heat of evaporation, J/kg
m	rate of water evaporation, kg/s
Q	heat rate, W
S	cross section area, m^2
T	temperature, °C
Z	bed height, m

Greek Symbols

ε	Effectiveness
ω	air specific humidity, kg_w / kg_{da}
ρ	density, kg/m^3
η	collector efficiency

Subscripts

a	Air
da	dry air
i	Inlet
L	Liquid
o	Outlet
max	Maximum

INTRODUCTION

Energy consuming is a strict issue in designing new refrigeration and air conditioning (R&AC) systems. Considerable attention has been given to R&AC systems in order to decrease its electricity consumption. Refrigeration and air conditioning equipment are inefficient energy saving due to design faults, bad installations, and lack of maintenance and are susceptible to fail up operation frequently. The energy saving is reached through the optimization of the equipment performance with the use of control techniques in these systems, [1-3].

Ayman A. etl., proposed an open solar absorption cooling system which is shown in Fig. 1 as efficient energy saving cooling system. The weak absorbent solution is heated and subsequently concentrated in the solar collector. The strong

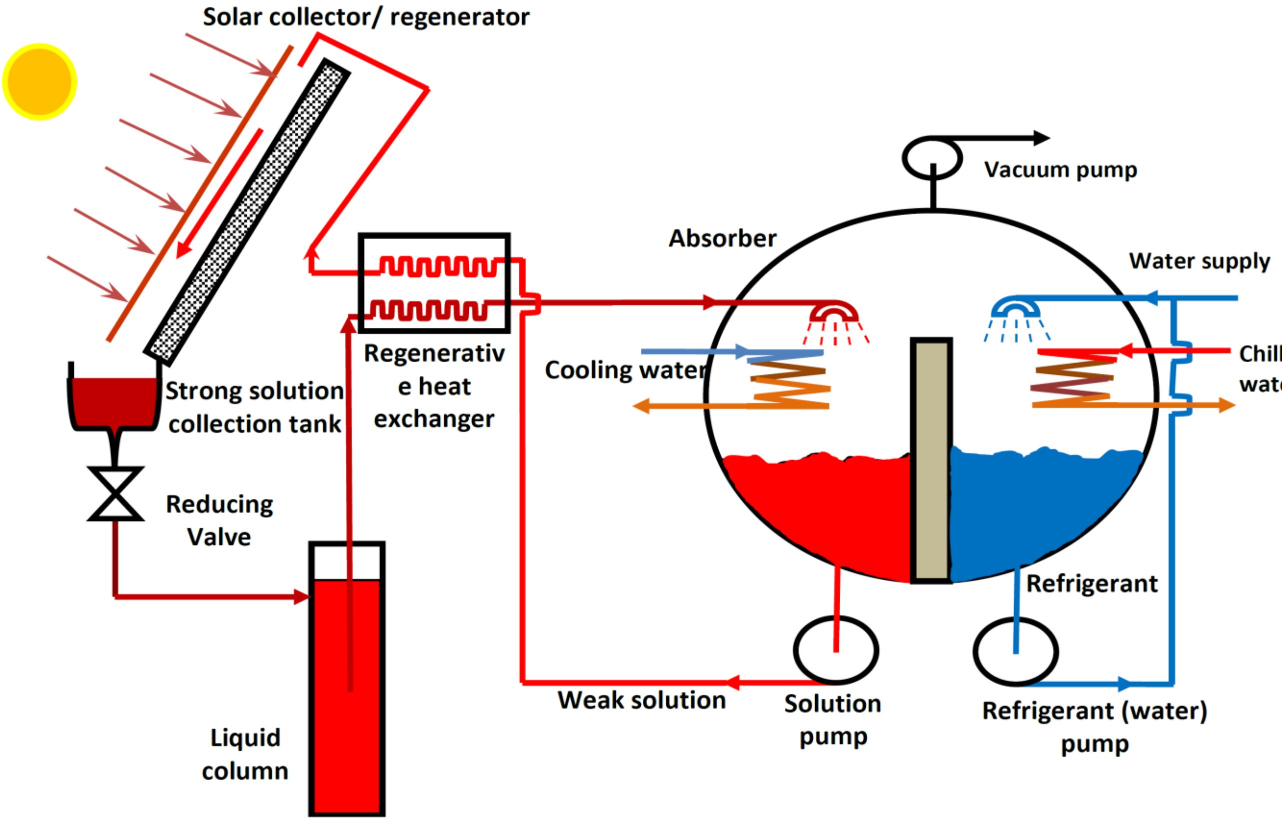

Figure 1: Schematic of the Solar –Powered Open Absorption Cooling System

regenerated solution leaves the collector and passes through a liquid column, to allow the strong solution to go from atmospheric pressure to reduced pressure efficiently. The strong solution then passes through a regenerative heat exchanger on its way to the absorber, where the strong solution absorbs water from the evaporator, maintaining the reduced pressure required with the energy supplied by heat from the cold space. The resultant weak solution is pumped from the absorber back to atmospheric pressure through the regenerative heat exchanger and the collector, completing the cycle, [4-5].

The advantages of this system would include a simpler collector, which also acts as a regenerator, and a reduction in thermal losses .The overall performance of the system is governed entirely by the rate at which water is driven from the solution in the collector, since this determined the flow of water that can be introduced into the evaporator as refrigerant. The rate of water evaporation from the regenerator gives a direct measure of the system cooling capacity.

However, there are dead-times related to fluid transportation which are variable depending on the operating conditions. Several control strategies have been tested at solar power plants to address these problems [7–9]. Model predictive controllers have also received a lot of attention in the last few decades, both within the research control community and in industry [10]. The basic idea is to calculate a sequence of future control signals in such a way that it minimizes a multistage cost function defined over a control horizon.

In this study, a DC motor is used to drive the generator pump in the heating cycle as it is described below and a second DC motor is used to drive the feed pump in the cooling cycle of a solar-powered refrigeration. Several techniques have been proposed in the literature for the direct conversion of the solar energy to heating, cooling or both.

Although refrigeration systems are designed to satisfy the maximum load, they work at partial load conditions most of their life cycle and they are regulated as on/off controlled. On-off control method is the most used conventional technique to control refrigeration systems. This method has a big drawback of undesired current peaks during its state transitions [9]. A strategy that could be used to overcome these problems is to use a controller with self-tuning algorithm. In general, conventional controllers cannot deal with nonlinear behaviors including uncertainties in system parameters, which may reduce the energy efficiency. To solve this problem a nonlinear controller based on fuzzy logic is proposed in this paper. The most important advantage of these algorithms is to enable solving control problems without any already-known mathematical model.

THEORETICAL MODEL

Solar Radiation Model

Any analysis of systems powered by solar energy should start with the research of the radiation data available in the region being studied. In the recent subsection, the total radiation incident on the tilted surface could be evaluated in terms of the location, day of the year and time of the day. The total perceived solar radiation can be estimated by the following relationship:

$$H_t = R_B I_B + C I_{Bn}\left(\frac{1+\cos s}{2}\right) + (I_B + I_d)\rho_g\left(\frac{1-\cos s}{2}\right) \qquad (1)$$

where, I_B is beam radiation on a horizontal surface, R_B is beam radiation tilt factor, I_{Bn} is beam radiation at normal incidence, W/m^2, I_d diffuse sky radiation, W/m^2, C is diffuse radiation factor, s is surface tilt angle, ρ_g is solar reflectance of the Earth's surface. The three terms in the above equation represent the direct, diffuse, and reflected components, respectively.

The terrestrial beam radiation within the atmosphere and on the earth's surface on a typical clear day is calculated by [10]:

$$I_{Bn} = A\exp\left(\frac{-B}{\sin\alpha}\right) = A\exp(-Bm) \qquad (2)$$

where, A and B are empirically determined values which represent the apparent solar radiation at air mass zero, W/m^2, and an apparent atmospheric extinction coefficient, α is the solar altitude angle, and m is the air mass. The altitude angle, α can be evaluated from the following expression:

$$\sin\alpha = \sin L \sin\delta + \cos L \cos\delta \cosh \qquad (3)$$

where L, δ and h are the latitude, declination and hour angles, respectively. The declination angle, δ can be calculated as a function of the day number, n as:

$$\delta = 23.45 \sin\left[\frac{360}{365}(284+n)\right] \qquad (4)$$

The hour angle is defined by

$$h = \pm\frac{1}{4}(\mathit{number\ of}\ \min\ \mathit{from\ local\ solar\ noon}) \qquad (5)$$

where the value of h is assumed positive in the afternoon period.

In Equation. (1), the diffuse solar radiation is estimated from:

$$H_d = C F_{ss} I_{Bn} \qquad (6)$$

where, F_{ss} = $0.5(1+\cos s)$ angle between the surface and the sky and s is the tilt angle of the solar collector. The beam radiation tilt factor, R_B is defined by:

$$R_B = \frac{H_{Bt}}{H_B} = \frac{\cos i}{\cos z} \qquad (7)$$

where H_{Bt}, H_B are the beam radiation on a tilted surface and on the horizontal surface, respectively. The incidence angle, i, and zenith angle z are calculated from the following expressions,

$$\cos i = \sin(L-s)\sin\delta + \cos(L-s)\cos\delta\cosh \qquad (8)$$

$$\cos z = \sin\alpha \qquad (9)$$

$$daylength = \frac{2}{15}\cos^{-1}(-\tan L \tan\delta) \qquad (10)$$

The solar radiation absorbed by the solution in the collector/regenerator can be obtained from

$$H_a = H_t(1-\rho)\tau\alpha \qquad (11)$$

where ρ and τ are the reflectance and transmittance of the glass cover on the collector surface and α is the regenerator absorptivity.

The steady-state energy balance equations for the open cycle regenerator-segment of unit width are written as [3]:

$$H_a dx = m_s dH_s + m_a dH_a + U_L(T_s - T_0) + m h_{fg} \qquad (12)$$

The energy balance for the air stream passing through the regenerator-segment is written as:

$$m_a dH_a = h_a(T_s - T_a)dx - h_s(T_a - T_0)dx \qquad (13)$$

The amount of water evaporated from the weak solution and the rate of mass transport are given by

$$m = 0.622\frac{m_a}{p_b}(p_a - p_{ai}) \qquad (14)$$

$$\frac{dm}{dx} = \beta(p_s - p_a) \qquad (15)$$

and the relation between the mass of evaporated water and solution flow rates is given by:

$$C_s = C_{si}/(1-\frac{m}{m_s}) \qquad (16)$$

The relationship between the solution temperature, concentration and vapour pressure is given by [11] as

$$p_s = a + bT_s + \frac{c}{C_s} \tag{17}$$

where a, b and c are empirical constants.

1-Effect of air mass flow rate

In order to analyze the effect of air mass flow rate on regeneration process, the solution mass flow rate is settled at 20 kg/hr and the range of air mass flow rate is considered in the range (10kg/hr-200 kg/hr), then the vapour pressure difference between the regenerated solution and flowing air is plotted versus the regenerator length. For a given regenerator length, the vapour pressure, which is the mass transfer potential, is directly proportional with the rate of water evaporation, when the mass transfer coefficient is assumed constant. As shown in Fig. 2**,** the vapour pressure difference has a maximum for a given length of the regenerator. The length at which the maximum rate of evaporation occurs increases with the air flow rate. It can be noted that the rate of evaporation

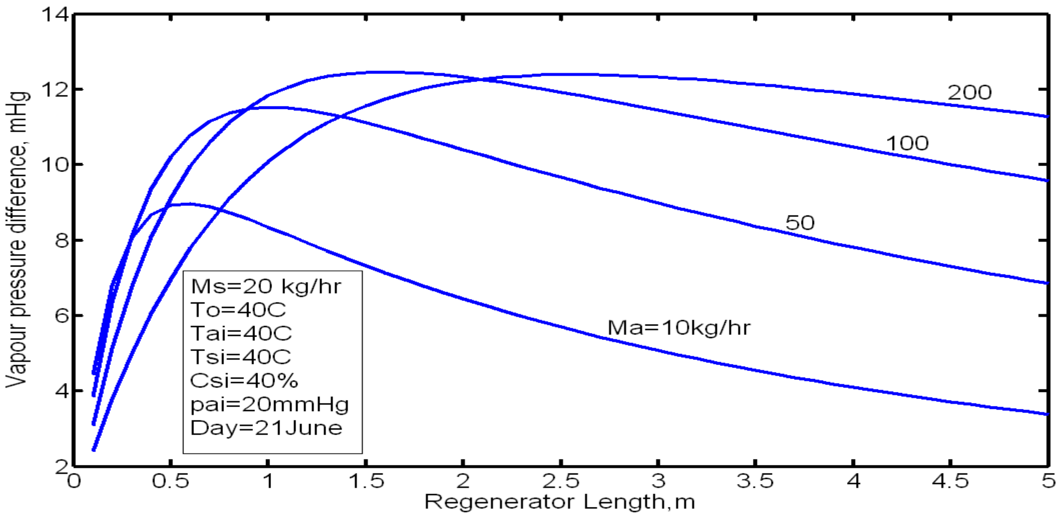

Figure 2: variation of vapour pressure at regenerator exit with at different values of air flow rate, at noon time

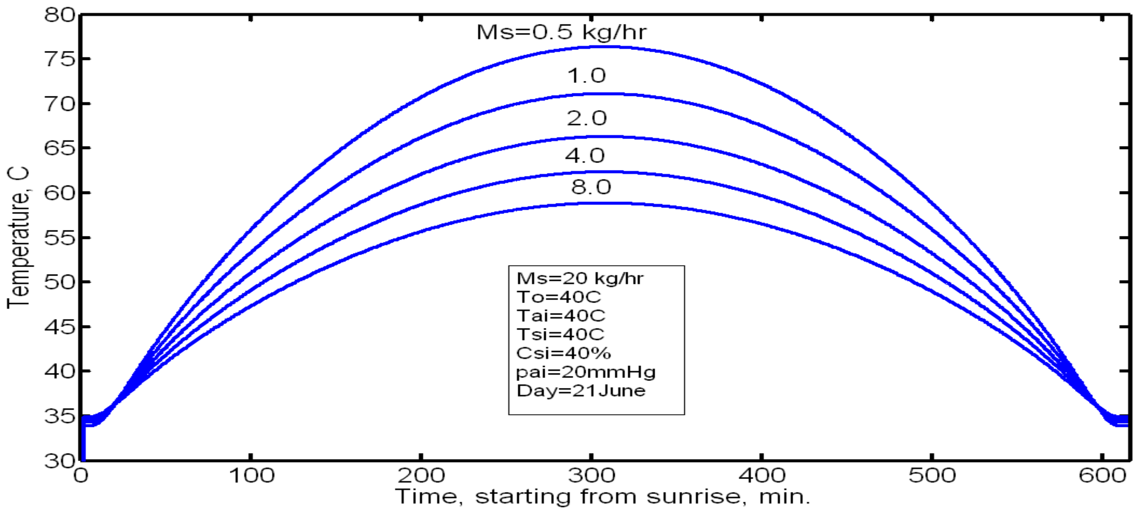

Figure 3: Variation of solution temperature during the day time at different values of solution flow rate

Concerning the effect of solution inlet concentration on regeneration process, the decrease of solution concentration can effectively improve regenerator performance, though it sacrifices solution outlet concentration.

2-Effect of solution flow rate

Figure 3 demonstrates the variation of the solution temperature during the regeneration period. This period starts from the sun rise to the set hour. As the solution flows from

International Journal of Applied Engineering Research ISSN 0973-4562 Volume 12, Number 24 (2017) pp. 14046-14053

the regenerator inlet to exit, it is expected that the solution temperature will be maximum at the end of the regenerator. On the other hand, the maximum temperature of the solution will follow the solar radiation intensity along the day time. It can be observed that the solution temperature increases with decrease in the flow rate.

The solution temperature at the end of regenerator (at noon time) is plotted versus regenerator length for different values of solution flow rate as shown in Fig.4 . It can be noted that the temperature increases gradually with regenerator length.

4-system coefficient of performance

The coefficient of performance, COP, of the system is illustrated in the surface plot shown in Fig. 5 For the specified operating conditions, a maximum value of the COP occurs at a given range of air flow rate and solution flow rate. However, the maximum value of COP is independent on the design parameters and operating conditions, therefore it is essential to select the design parameters for each ambient condition to maximize the COP of the system.

The implementation of a fuzzy logic controller for a solar refrigeration system and its advantages are illustrated in the next section.

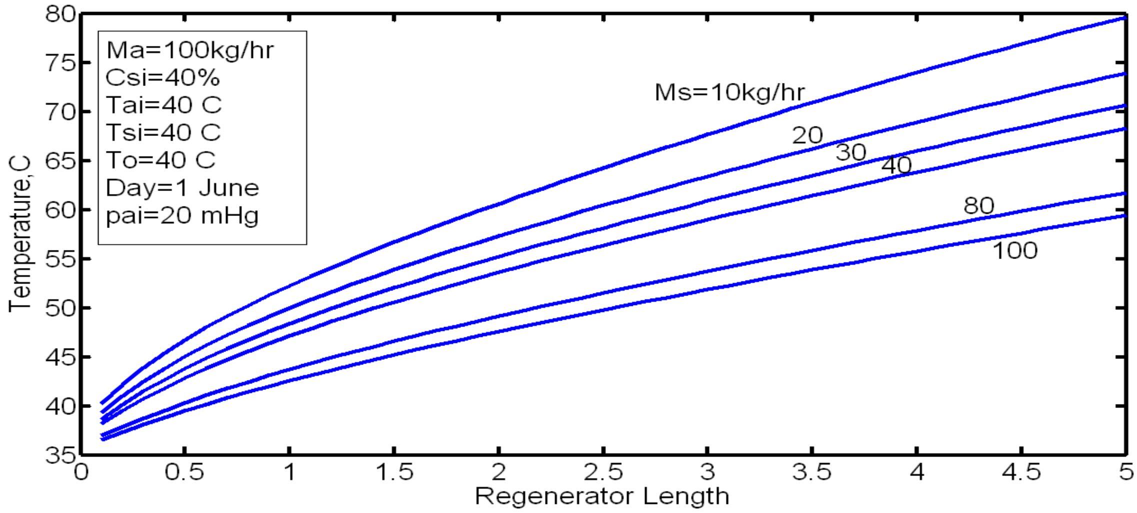

Figure 4: variation of solution temperature at regenerator exit at different values of air flow rate ,at noon time.

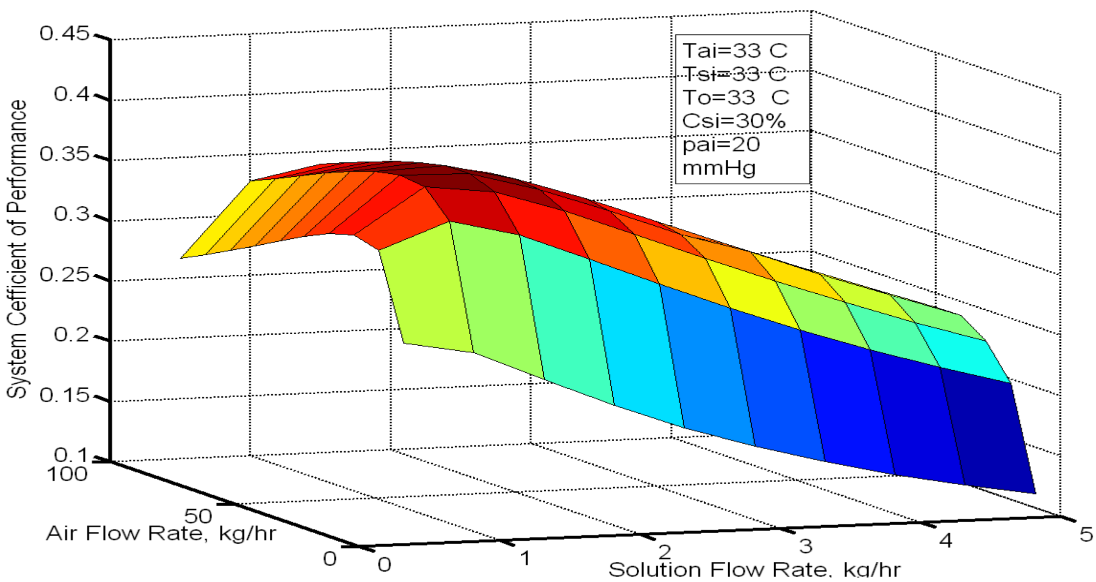

Figure 5: Surface plot showing the variation of system COP with air and solution flow rates

CONTROL DESIGN

In principle, the proposed design for the solar refrigeration system can be characterized by the refrigerant temperatures leaving the condenser and leaving the storage tank. A proper regulation of these state variables and their dynamic behavior can lead to more energy-efficient operations. The minimization problem for refrigerant temperature leaving the condenser is then formulated through the determination of controlled variables, subject to constraints. Here, the aim is to minimize the refrigerant temperature leaving the condenser in order to increase the system COP. To control the refrigerant flow rate from the feed pump and the generator pump, two dc motor which drive these pumps should be controlled their position effectively. Two DC motors are used to drive the generator pump and the feed pump of the system. The command signal for the first DC motor driving the Feed Pump is the pressure measured in the Generator's output while the command signal for the DC motor driving the Generator Pump, is the oil temperature measured in the solar panel output. In Fig. 6, the block diagram for each DC motor controller is shown. A tacho-generator is used in the feedback for the actual speed reading. There is a linear relation between the voltage of the tacho-generator output waveform and the rotational speed of the motor shaft.

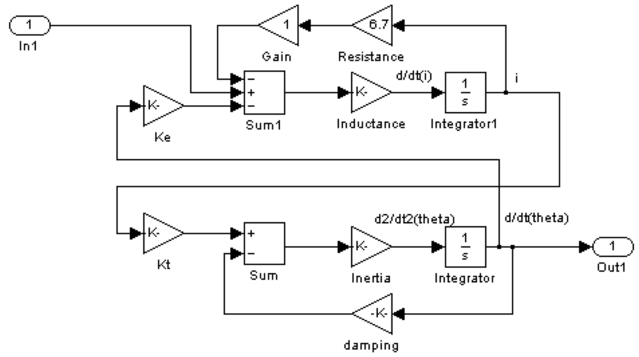

Figure 6: DC motor model.

.

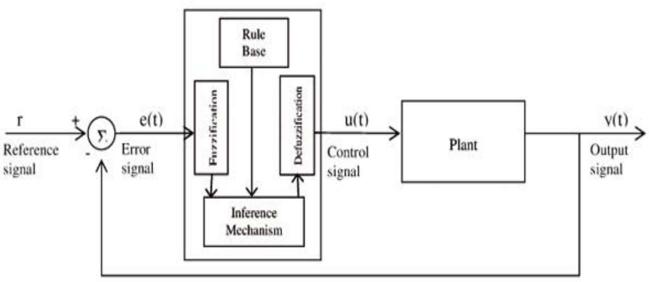

Figure 7: Detail of a control system with fuzzy logic controller

There are a number of different ways to implement the fuzzy inference engine. Among the very first such proposed techniques is that due to Mamdani [10], which describes the inference engine in terms of a fuzzy relation matrix and uses the compositional rule of inference to arrive at the output fuzzy set for a given input fuzzy set. The output fuzzy set is subsequently defuzzified to arrive at a crisp control action. A review of ranging inferencing techniques is given by Kosko [11]. The inference methodology we employ here is discussed in [12]. A proposed fuzzy logic control is illustrated in Fig.7 and its flow chart is shown in Fig.8.

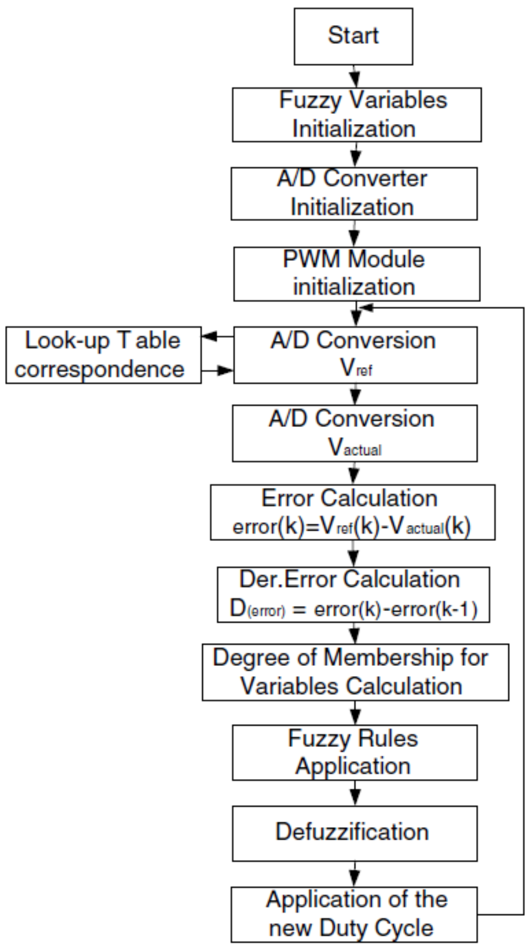

Figure 8: Flow chart of the implementation of fuzzy controller

Let the input variables be e_p for $1 \le p \le P$. The i^{th} membership function in the fuzzifier corresponding to the p^{th} input is $\{\mu_p^i | 1 \le i \le N_p\}$. We denote the single output by f, with corresponding defuzzification membership functions $\{v^g | 1 \le g \le G\}$.

Generalization of inference and adaptation techniques to more than one output is straightforward. In the following analysis, for DC motor position control system, we consider $P = 2$. Defining $N_p = N$ for $p = 1$, and $N_p = M$ for $p = 2$, for a given output membership function v^g, the rules are of the form:

International Journal of Applied Engineering Research ISSN 0973-4562 Volume 12, Number 24 (2017) pp. 14046-14053
© Research India Publications. http://www.ripublication.com

$$\textit{if } e_1 \textit{ is } \mu_1^i \textit{ and } e_2 \textit{ is } \mu_2^j \textit{ OR} e_1 \textit{ is } \mu_1^l \textit{ and } e_2 \textit{ is } \mu_2^m \textit{ OR}.... \\ \textit{Then}....... f \textit{ is } v^g$$

Define a set

$$S_g = \{l, m \mid \mu_1^l \textit{ and } \mu_2^m \textit{ are antecedents of a rule with consequent } v^g\} \tag{18}$$

The familiar operations to arrive at the output are as follows:

1. Perform a pair wise fuzzy intersection *T*, on each of the membership values of e_1 and e_2 in μ_1^l and μ_2^m for every rule with consequent v^g, forming activation values ζ:

$$\zeta_{lm}^g = \underset{l.m \in S_g}{T} \left(\mu_1^l(e_1) - \mu_2^m(e_2) \right) \tag{19}$$

Let us assume that the (*T*-norm) operator *T* itself is parameterized by α, i.e., $T = T(\alpha)$.

2. Collect activation values for like output membership functions and perform a fuzzy union T^*, where $T^* = T^*(\beta)$

$$w_g = \underset{l,m \in S_g}{T} \left(\zeta_{lm}^g \right) \tag{20}$$

3. These values are defuzzified to generate the output estimated value, $f(e_1, e_2)$, by computing the centroid of the composite membership function μ:

$$\mu = \sum_{g=1}^{G} w_g v^g \tag{21}$$

$$y(e_1, e_2) = \frac{\sum_{g=1}^{G} w_g C_g A_g}{\sum_{g=1}^{G} w_g A_g} \tag{22}$$

where

$$A_g = \int v^g(e)de; \; C_g = \frac{\int e v^g(e) de}{\int v^g(e) de} \tag{23}$$

A_g and C_g are, respectively, the area and centroid of the consequent membership function v^g.

The fuzzifier and defuzzification stages requires choice of

- The number of membership functions.
- The shape of membership functions.
- A measure of central tendency of the consequent altered output membership functions. The center of mass is typically used, although use of medians and modes can also be used to arrive at the crisp output.

It is thus seen that both the fuzzification and defuzzification stages require choices of cardinality, position and shape of membership functions. The defuzzification operation itself can be parameterized, and the inference engine requires choices to be made among numerous fuzzy aggregation operators, which could be parameterized.

As part of the fuzzy design categories, we present a technique for choosing the shape of membership functions, as well as a broad methodology for tuning generalized aggregation operators in a fuzzy inference system.

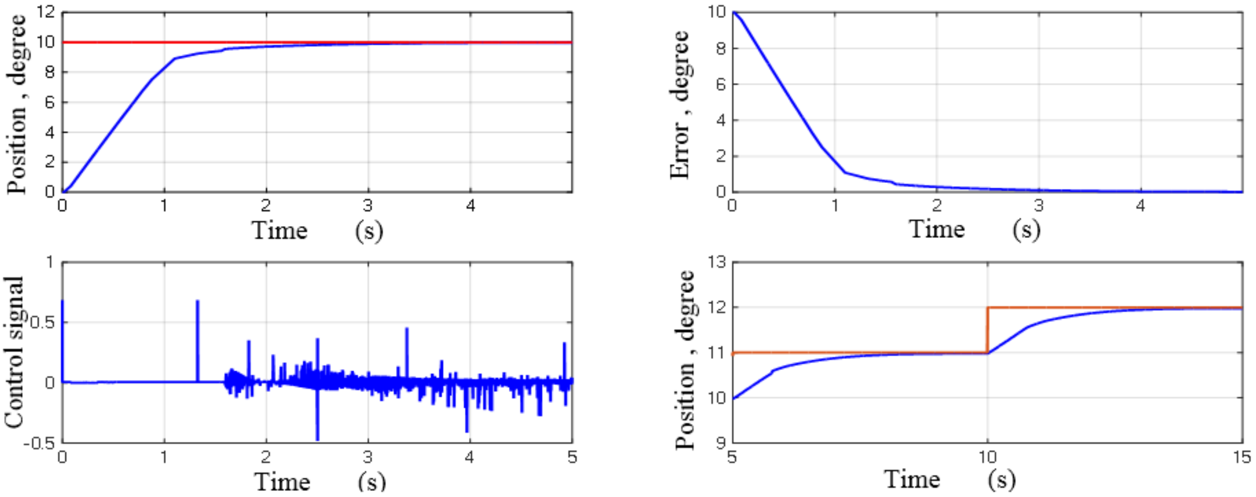

Figure 9-a the system response to step input of 10°. **Figure 9-b.** the error signal due to the step input.
Figure 9-c. the normalized crossponding control signal **Figure 9-d.** the response with change of the step input by 10%.

The design of the system has been followed by the computer simulation using the Matlab/Simulink software to simulate the closed-loop control system. the simulation is performed in the time domain and the sampling period is set at T=5 ms. The control algorithm described has been used to drive the main two dc motors (the generator pump and the feed pump) of the solar refrigeration system.

The step response based on the proposed fuzzy controller is illustrated in Fig.9-a. the response has no overshoot with settling time less than 3 sec. and steady state error nearly zero as shown in Fig. 9-b. while its normalized control signal is shown in Fig. 9-c. To check the system robustness, sudden change which is illustrated in Fig.9-d and applied to the system by increase the input signal 10% and the controller adapt the response to follow the new reference.

CONCLUSION

The performance of a solar-powered desiccnt regenerator has been investigated. Also an intelligent fuzzy logic controller to adjust the rotational speed of two DC motors of a solar refrigerant system has been described in this paper. Fuzzy logic controller is implemented using a general purpose low-cost microcontroller for the position control of DC motors. The controller can be implemented by using only a small amount of components.

The implementation of fuzzy logic control techniques shows that fuzzy logic can reduce the effects of nonlinearities in a DC motor and improve the performance of the controller. Finally, fuzzy logic controller algorithm can be easily transferred to different motor sizes and allows a strong tolerance for electric motor parameter oscillations. It is also concluded that the proposed model can be successfully used for predicting the overall performance of the system.

ACKNOWLEDGEMENTS

This study is supported by Taif University under a contract NO. 1-438-5588. The University is highly acknowledged for the financial support.

REFERENCES

[1] H. Factor, G.A. Grossman, A packed bed dehumidifier/regenerator for solar air conditioning with liquid desiccant, Solar Energy 24 (1980) 541–550.

[2] Gandhidasan P. Simple analysis of a forced flow solar regeneration system. Energy 1981;6(6):436–7.

[3] S. Alizadeh and W. Y. Saman, "Modeling and performance of a forced flow solar collector/regenerator using liquid desiccant," *Solar Energy*, vol. 72, No. 2, pp. 143-154, 2002.

[4] P. Gandhidasan, "A simple analysis of an open regeneration system," *Solar Energy*, vol. 31, No. 3, pp. 343–5, 1983.

[5] Y. Saito, "Regeneration characteristics of adsorbent in the integrated desiccant/collector," Trans. ASME J Solar Energy Engineering, vol. 115, pp. 169–175, 1993.

[6] D. J. Nelson and B. D. Wood, "Evaporation rate model for a natural convection glazed collector/regenerator," *Trans. ASME J Solar Energy Engineering*, vol. 112, pp. 51–57, 1990.

[7] R. Yang and P. L. Wang, "Experimental study of a forced convection solar collector/regenerator for open cycle absorption cooling," Trans. ASME J Solar Energy Engineering, vol. 116, pp. 194-199, 1994.

[8] Kabeel AE. Augmentation of the performance of solar regenerator of open absorption cooling system. Renewable Energy 2005;30(3):327–38.

[9] Kakabayev A. and Khandurdyev (1969) Absorption solar regeneration unit with open regeneration of solution. Geliotekhnika 1969;5(4):28–32.

[10] K. Jui Sheng Hsieh, Solar Energy Engineering, Prentice- Hall, Inc., Englewood Cliffs, New Jersey, USA, 1986.